Dalton Transactions

Accepted Manuscript

This is an *Accepted Manuscript*, which has been through the Royal Society of Chemistry peer review process and has been accepted for publication.

Accepted Manuscripts are published online shortly after acceptance, before technical editing, formatting and proof reading. Using this free service, authors can make their results available to the community, in citable form, before we publish the edited article. We will replace this *Accepted Manuscript* with the edited and formatted *Advance Article* as soon as it is available.

You can find more information about *Accepted Manuscripts* in the Information for Authors.

Please note that technical editing may introduce minor changes to the text and/or graphics, which may alter content. The journal's standard Terms & Conditions and the Ethical guidelines still apply. In no event shall the Royal Society of Chemistry be held responsible for any errors or omissions in this *Accepted Manuscript* or any consequences arising from the use of any information it contains.

ROYAL SOCIETY OF CHEMISTRY

www.rsc.org/dalton

Crystal structure and magnetic properties of 3-pyridinecarboxylate-bridged Re(II)M(II) complexes (M = Cu, Ni, Co and Mn)

Mario Pacheco[a], Alicia Cuevas[a], Javier González-Platas[b], Francesc Lloret[c], Miguel Julve[c], Carlos Kremer[a,*]

[a] Cátedra de Química Inorgánica, Departamento Estrella Campos, Facultad de Química, Universidad de la República, Avda. General Flores 2124, Montevideo, Uruguay.

[b] Departamento de Física, Servicio de Difracción de Rayos X. Universidad de La Laguna, Tenerife, Spain

[c] Instituto de Ciencia Molecular, Universidad de Valencia, C/ Catedrático José Beltrán 2, 46980 Paterna, Valencia, Spain.

* Corresponding author, email: ckremer@fq.edu.uy

Abstract

The novel Re(II) complex $NBu_4[Re(NO)Br_4(Hnic)]$ (**1**) and the heterodinuclear compounds $[Re(NO)Br_4(\mu\text{-nic})Ni(dmphen)_2]\cdot\frac{1}{2}CH_3CN$ (**2**), $[Re(NO)Br_4(\mu\text{-nic})Co(dmphen)_2]\cdot\frac{1}{2}MeOH$ (**3**), $[Re(NO)Br_4(\mu\text{-nic})Mn(dmphen)(H_2O)_2]\cdot dmphen$ (**4**), $[Re(NO)Br_4(\mu\text{-nic})Cu(bipy)_2]$ (**5**) $[Re(NO)Br_4(\mu\text{-nic})Cu(dmphen)_2]$ (**5'**) (NBu_4^+ = tetra-*n*-butylammonium cation, Hnic = 3-pyridinecarboxylic acid, dmphen = 2,9-dimethyl-1,10-phenanthroline, bipy = 2,2'-bipyridine) have been prepared and the structures of **1**-**5** determined by single crystal X-ray diffraction. The structure of **1** consists of $[Re(NO)Br_4(Hnic)]^-$ anions and NBu_4^+ cations. Each Re(II) is six-coordinate with four bromide ligands, a linear nitrosyl group and a nitrogen atom from the Hnic molecule, in a distorted octahedral surrounding. The structures of **2**-**5** are made up of discrete heterodinuclear Re(II)M(II) units where the fully deprotonated $[Re(NO)Br_4(nic)]^{2-}$ entity acts as a didentate ligand through the carboxylate group towards the $[Ni(dmphen)_2]^{2+}$ (**2**), $[Co(dmphen)_2]^{2+}$ (**3**), $[Mn(dmphen)(H_2O)_2]^{2+}$ (**4**) and $[Cu(bipy)_2]^{2+}$ (**5**) fragments, the Re-M separation across the nic bridge being 7.8736(8) (**2**), 7.9632(10) (**3**), 7.7600(6) (**4**) and 8.2148(7) Å (**5**). The environment of the Re(II) ion in **2**-**5** is the same as in **1** and all M(II) are six-coordinate in highly distorted octahedral surroundings, the main source of the distortion being due to the reduced bite of the chelating carboxylate. The magnetic properties of **1**-**5'** were investigated in the temperature range 1,9-300 K. **1** behaves as a quasi magnetically isolated spin doublet with very weak antiferromagnetic interactions through space Br···Br contacts. Its magnetic susceptibility data were successfully modeled through a deep analysis of the influence of the ligand field, spin-orbit coupling, tetragonal distortion and covalence effects as variable parameters. Compounds **2**-**5'** exhibit weak antiferromagnetic interactions. The intramolecular exchange pathway in this family being discarded because of the symmetry of magnetic orbital of the Re(II) ion (d_{xy}) precludes any spin delocalization on the bridging nic orbitals, the observed magnetic interactions are most likely mediated by π-π type interactions between the peripheral

Dalton Transactions Accepted Manuscript

ligands which occur in them. Only in the case of **4**, short through space Br···Br contacts of ca. 4.03 Å (values larger than 5.5 Å in 2, **3** and **5**) could be involved in the exchange coupling.

Introduction

The preparation and full characterization of stable Re(II) mononuclear complexes has been the subject of a previous report by us.[1] Stability of this less-common rhenium oxidation state has been achieved by using the $[Re(NO)]^{3+}$ core which provides the basis of octahedral complexes like $NBu_4[Re(NO)Br_4(EtOH)]$ (NBu_4^+ = tetra-*n*-butylammonium cation) which can be substituted in the *trans* position by releasing an ethanol molecule. Four complexes of general formula $NBu_4[Re(NO)Br_4(L)]$ [L = pyridine (py), pyrazine (pyz), pyrimidine (pym) and pyridazine (pyd)] have been obtained by this synthetic route. With the characterization of these compounds, it was possible to perform a detailed study of their magnetic properties. Re(II) ion has an outer $5d^5$ shell in a low spin configuration, and the magnetic behavior of its complexes was scarcely described. Early reports on the magnetism of this ion showed an unusual behavior with a strong temperature-independent paramagnetism (TIP) [values in the range χ_{TIP} = (1.4 – 1.8) x 10^{-3} cm^3 mol^{-1}] and a small *g*-factor.[2] We also developed a theoretical formalism which included the influence of the ligand field, spin-orbit coupling, axial distortion, and covalence effects as variable parameters to treat the magnetic data of this family of mononuclear Re(II) complexes.[1]

Once the magnetic behavior of the Re(II) complexes is reasonably well understood, the next step is to study systematically, for the first time, the exchange coupling between this 5d metal ion and other 3d paramagnetic ions. We and others have already focused on this subject in the case of Re(IV) polynuclear complexes (representative papers are presented in refs. [3-7]). The magnetic interaction in these compounds was found to be ferro- or antiferromagnetic depending on the orthogonality or non-orthogonality between the interacting magnetic orbitals through the chemical bridge.

On the basis of previous results concerning the stable complexes of py, pyz, pym, and pyd ligands with the $[Re(NO)]^{3+}$ core,[1] we decided to explore the use of 3-pyridinecarboxylic acid (nicotinic acid, Hnic) as potential bridge to prepare heterobimetallic Re(II)-M(II) systems [M(II) = first-row transition metal ion) having in mind that the presence of an heterocyclic nitrogen atom in Hnic together with the carboxylic group would afford nicotinate bridged heterodinuclear compounds in a straightforward manner (see Chart 1).

Our approach involves the synthesis of the mononuclear $[Re(NO)Br_4(Hnic)]^-$ complex as the $(NBu_4)^+$ salt. In a second step, the ability of this complex to act as a ligand against partially blocked metal complexes was checked. Our first results along this line afforded the compounds of formula $NBu_4[Re(NO)Br_4(Hnic)]$ (**1**) and the heterodinuclear compounds $[Re(NO)Br_4(\mu\text{-nic})Ni(dmphen)_2]\cdot$ ½CH_3CN (**2**), $[Re(NO)Br_4(\mu\text{-nic})Co(dmphen)_2]\cdot$ ½MeOH (**3**), $[Re(NO)Br_4(\mu\text{-nic})Mn(dmphen)(H_2O)_2]\cdot$dmphen (**4**), $[Re(NO)Br_4(\mu\text{-nic})Cu(bipy)_2]$ (**5**) $[Re(NO)Br_4(\mu\text{-nic})Cu(dmphen)_2]$ (**5'**) (Hnic = 3-pyridinecarboxylic acid, dmphen = 2,9-dimethyl-1,10-phenanthroline and bipy = 2,2'-bipyridine). Their preparation and magneto-structural investigation are the subject of this work.

Dalton Transactions Accepted Manuscript

Experimental

Materials

Hnic, dmphen, 2,2´-bipy, $Ni(ClO_4)_2{\cdot}6H_2O$, $Co(ClO_4)_2{\cdot}6H_2O$, $Mn(ClO_4)_2{\cdot}6H_2O$, $Cu(CF_3SO_3)_2$ and solvents employed in the synthesis were purchased from commercial sources and used as received. $NBu_4[Re(NO)Br_4(EtOH)]$ was prepared from $KReO_4$ and NO as previously reported.[1]

Synthesis of the complexes

$NBu_4[Re(NO)Br_4(Hpyc)]$ (**1**)

A mixture of $NBu_4[Re(NO)Br_4(EtOH)]$ (50 mg, 0.061 mmol) and an excess of nicotinic acid (113 mg, 0.918 mmol) in 20 mL of an i-PrOH/acetone mixture (4:1 v/v) was stirred and heated at 50 °C for 5 hours leading to a deep yellow solution. After cooling at room temperature, the mixture is evaporated to dryness. The solid residue is redissolved in 5 mL of acetone and the nicotinic acid (insoluble in acetone) is filtered and discarded. 5 mL of isopropanol are poured into the mother liquor and the mixture is allowed to evaporate at room temperature. X-ray quality crystals, as green polyhedral, were grown from this solution after one week. Yield (based on Re): 51 %. Found: C, 29.83; H, 4.92; N, 4.85. Anal. calcd for $C_{22}H_{41}Br_4N_3O_3Re$ (**1**): C, 29.31; H, 4.58; N, 4.66. IR(KBr/cm^{-1}): bands associated to the nicotinic acid appear at 3448w [ν(O-H)], 1716s [ν(C=O)], 1058m [ν(C-OH)], 748m [ν(C-COOH)], 1610m, 1471s, 1295s, 1205m and 689s (pyridine ring vibrations) and 1769vs [ν(NO)].

$[Re(NO)Br_4(\mu\text{-nic})Ni(dmphen)_2]{\cdot}½CH_3CN$ (**2**)

A solid sample of **1** was dissolved in 20 mL of MeCN and poured into another acetonitrile solution (16 mL) containing $Ni(ClO_4)_2{\cdot}6H_2O$ (20.1 mg, 0.055 mmol) and dmphen (23.1 mg, 0.111 mmol) at room temperature. A green crystalline solid separated after 12 days. It was filtered and dried in the air. Some of the crystals were suitable for X-ray diffraction. Yield (based on Re): 57%. Found: C, 37.85; H, 2.64; N, 8.17. Anal. calcd for $C_{35}H_{29.5}Br_4N_{6.5}NiO_3Re$ (**2**): C, 36.44; H, 2.58; N, 7.89. IR (KBr/cm^{-1}): 1058w [ν(C-O)], 731m [ν(C-COO)], 1616m [ν_{as}(C-O-O)], 1409m [ν_s(C-O-O)], 1293w, 1200m and 692w (pyridine ring vibrations) and 1753vs [ν(NO)].

$[Re(NO)Br_4(\mu\text{-pyc})Co(dmphen)_2]{\cdot}½MeOH$ (**3**)

A solid sample of **1** (10 mg, 0.011 mmol) was dissolved in 20 mL of MeOH. This solution was poured into anther acetonitrile solution (16 mL) containing $Co(ClO_4)_2{\cdot}6H_2O$ (20.3 mg, 0.055 mmol) and dmphen (23.1 mg, 0.111 mmol) at room temperature. A greenish-brown crystalline solid separated after four days. It was filtered and dried in the air. Suitable crystals for X-ray diffraction were found in this crop. Yield (based on Re): 70 %. Found: C, 36.28; H, 2.57; N, 7.60. Anal. calcd for $C_{34.5}H_{30}Br_4CoN_6O_{3.5}Re$ (**3**): C, 36.05; H, 2.63; N, 7.31. IR (KBr/cm^{-1}): 1056w [ν(C-O)], 731m [ν(C-COO)], 1618s [ν_{as}(C-O-O)], 1396m [ν_s(C-O-O)], 1293w, 1293w and 692w (pyridine ring vibrations) and 1757vs [ν(NO)].

Dalton Transactions Accepted Manuscript

$[Re(NO)Br_4(\mu\text{-nic})Mn(dmphen)(H_2O)_2]\cdot dmphen$ (**4**)

A solid sample of **1** (10 mg, 0.011 mmol) dissolved in 20 ml of EtOH. This solution was poured into a second ethanolic solution (20 mL) containing $Mn(ClO_4)_2\cdot 6H_2O$ (19.9 mg, 0.055 mmol) and dmphen (23.1 mg, 0.111 mmol) at room temperature. Then 500 µL of DMF were added. After 10 days a green crystalline solid is formed. It was filtered and dried in the air. Some of these crystals were suitable for X-ray diffraction. Yield (based on Re): 48 %. Found: C, 36.13; H, 2.59; N, 7.01. Anal. calcd for $C_{34}H_{32}Br_4MnN_6O_5Re$ (**4**): C, 35.04; H, 2.77; N, 7.21. IR (KBr/cm^{-1}): 1057vw [ν(C-O)], 731m [ν(C-COO)], 1617m [ν_{as}(C-O-O)], 1405m [ν_s(C-O-O)], 1291w, 1200m and 695w (pyridine ring vibrations) and 1755vs [ν(NO)].

$[Re(NO)Br_4(\mu\text{-nic})Cu(bipy)_2]$ (**5**)

A solid sample of **1** (10 mg, 0.011 mmol) was dissolved in 20 mL of MeCN. This solution was poured into an ethanolic solution (20 mL) containing $Cu(CF_3SO_3)_2$ (19.8 mg, 0.055 mmol) and 2,2'-bipyridine (17.3 mg, 0.111 mmol) at room temperature. Then, 500 µL of DMF was added. A green crystalline solid is formed after 12 days. It was filtered and dried in the air. Crystals suitable for X-ray diffraction were found in this crop. Yield (based on Re): 52 %. Found: C, 30.30; H, 1.90; N, 7.91. Anal. calcd for $C_{26}H_{20}Br_4CuN_6O_3Re$ (**5**): C, 30.21; H, 1.95; N, 8.13. IR (KBr/cm^{-1}): 1058m [ν(C-O)], 732m [ν(C-COO)], 1620m [ν_{as}(C-O-O)], 1375m [ν_s(C-O-O)], 1313m, 1200m and 695m (pyridine ring vibrations) and 1757s [ν(NO)].

$[Re(NO)Br_4(\mu\text{-nic})Cu(dmphen)_2]$ (**5'**)

A solid sample of **1** (10 mg, 0.011 mmol) was dissolved in 20 mL of MeCN. This solution was poured into a second solution (15 mL) $Cu(OSO_2CF_3)_2$ (19.8 mg, 0.055 mmol) and dmphen (23.1 mg, 0.111 mmol) in EtOH at room temperature. After 1 week a green solid is formed. Crystals were filtered, washed with EtOH (2 x 5 mL) and dried in the air. Our attempts to obtain single crystals from different solvents (EtOH, MeOH, i-prOH, acetone, CH_3CN) and solvent combinations were unsuccessful. Yield (based on Re): 78%. Found: C, 35.74; H, 2.40; N, 7.07. Anal. calcd for $C_{34}H_{29}Br_4CuN_6O_3Re$: C, 35.85; H, 2.57; N, 7.38. IR (KBr/cm^{-1}): 1049w [ν(C-O)], 730m [ν(C-COO)], 1623s [ν_{as}(C-O-O)], 1355m [ν_s(C-O-O)], 1294w, 1196m, 697m (pyridine ring vibrations) and 1760s [ν(NO)].

Physical techniques

The IR spectra were recorded on a Bomen MB FT–IR spectrophotometer in the range 4000-400 cm^{-1}. Elemental analysis (C, H, N) was accomplished on a Flash 2000 (Thermo Scientific) elemental analyzer. X-band EPR spectra on polycrystalline samples were performed at different temperatures with a Bruker ER 200 spectrometer equipped with a helium continuous-flow cryostat. The value of the X-band EPR frequency is 9.475 GHz. Magnetic susceptibility measurements on polycrystalline samples were carried out with a Superconducting Quantum Interference Design (SQUID) magnetometer in the temperature range 1.9–300 K. In order to

Dalton Transactions Accepted Manuscript

avoid saturation phenomena, we used external dc magnetic fields of 250 G (T < 50 K) and 5000 G (T ≥ 50 K). Diamagnetic corrections of the constituent atoms were carefully estimated from Pascal's constants [χ_{dia} = –460 x 10^{-6} (**1**), –590 x 10^{-6} (**2**), –485 x 10^{-6} (**3**), –595 x 10^{-6} (**4**), –520 x 10^{-6} (**5**), –470 x 10^{-6} cm^3 mol^{-1} (**5'**)] [9a]. Experimental susceptibilities were also corrected for the temperature independent paramagnetism of the metal ions [χ_{tip} = 150 x 10^{-6} (**2**), 90 x 10^{-6} (**3**), 300 x 10^{-6} (**4**), 60 x 10^{-6} cm^3 mol^{-1} (**5** and **5'**)] [9b] as well as for the magnetization of the sample holder previously measured in the same conditions.

X-Ray data collection and structure refinement

X-ray diffraction data on single crystals of **1**-**5** were collected with an Agilent SuperNOVA diffractometer with microfocus X-ray using Cu Kα radiation (λ = 1.54184 Å). CrysAlisPro[10] software was used to collect, index, scale and apply a numerical absorption correction based on Gaussian integration over a multifaceted crystal model. The structures were solved by charge-flipping algorithm using Superflip program[11]. Fourier recycling and least-squares refinement were used for the model completion with SHELXL-2014[12]. All non-hydrogen atoms were refined with anisotropic thermal parameters using full-matrix least-squares procedures on F^2. All hydrogen atoms were allowed to ride on their parent atoms with $U_{iso}(H) = 1.2U_{eq}(C)$ and $U_{iso}(H) = 1.5U_{eq}(C)$ for the methyl groups.

The acetonitrile (**2**) and methanol (**3**) molecules have been refined using a fixed occupancy factor of 0.5. The NO group in the structure of **5** also manifested this slight disorder.

The geometrical analysis of the interactions in the structures was performed with PLATON[13] and Olex2[14] programs. Crystal data, collection procedures and refinement results are summarized in Table 1 (**1**-**5**) and selected bond lengths and angles are listed in Tables 2 (**1**), 3 (**2** and **3**), 4 (**4**) and 5 (**5**).

Crystallographic data for the structures reported in this contribution have been deposited with the Cambridge Crystallographic Data Centre as supplementary publication 1055519-1055523. Copies of the data can be obtained free of charge on application to the CCDC, Cambridge, U.K. (http://www.ccdc.cam.ac.uk/).

Results and discussion

Short description of the preparation of the complexes

The $[Re(NO)Br_4(EtOH)]^-$ complex has been successfully used as a precursor for other Re(II) complexes. The *trans* effect produced by the NO group[15], makes easy the replacement of the ethanol ligand by other molecules like nicotinic acid under mild conditions, according to the reaction:

$$[Re(NO)Br_4(EtOH)]^- + Hnic \rightarrow [Re(NO)Br_4(Hnic)]^- + EtOH$$

Dalton Transactions Accepted Manuscript

The incoming Hnic ligand does not undergo any deprotonation upon its coordination to the Re(II) and the resulting complex keeps its initial negative charge. The IR spectra of **1** is characterized by a strong absorption at 1769 cm^{-1} corresponding to the stretching mode of the nitrosyl group and two bands at 1610 (m) and 1716 (vs) cm^{-1} from the carboxylic group of the Hnic ligand.

The second step of the synthesis was to use **1** as a metalloligand towards preformed 3d metal complexes whose coordination sphere is unsaturated. These assembling reactions afforded the heterobimetallic compounds **1**-**5** and **5'**. The IR spectra show that the NO group is not altered during the formation of the heterodinuclear compounds, the ν(NO) band appearing at 1753 (**2**), 1756 (**3**), 1755 (**4**), 1757 (**5**) and 1760 cm^{-1} (**5'**). Complexes **2**–**4** exhibit values of Δ [$\nu_a(COO^-)$ – $\nu_s(COO^-)$] in the expected range for chelating carboxylate complexes [207 (**2**), 222 (**3**) and 212 cm^{-1} (**4**)] whereas they are 245 (**5**) and 268 cm^{-1} for **5** and **5'** respectively, suggesting an asymmetric bidentate nicotinate ligand for these latter compounds.[16]

Description of the structures

NBu_4[Re(NO)Br_4(Hpyc)] (1). The structure of **1** consists of mononuclear [Re(NO)Br_4(Hnic)]$^-$ complex anions and bulky NBu_4^+ cations in a 1:1 molar ratio (Figure 1). Two crystallographically independent [Re(NO)Br_4(Hnic)]$^-$ units occur in **1** but their structures are quite similar, in particular the coordination geometry around the rhenium(II) ions (Re1A and Re1B, see Table 2). Each anion contains a rhenium center in a distorted octahedral environment, being surrounded by four bromide anions, one NO group and a pyridine-nitrogen from the Hnic molecule, these last two ligands being in *trans* position. The Re–N(O) bond distances are 1.743(6) and 1.738(5) Å and Re–N(Hnic) bond lengths are 2.226(4) and 2.228(4) Å for Re1A and Re1B, respectively. The Re–Br bonds fall within the range 2.5073(9)–2.5255(9) Å [average values are 2.5179 (Re1A–Br) and 2.5169 Å (Re1B–Br)]. All these values agree well with those found in the literature for other Re(II) nitrosyl compounds.[1, 15, 17-19] The Re–NO group is practically linear [176.9(7) and 179.7(7)° for O1A–N1A–Re1A and O1B–N1B–Re1B, respectively] and the three atoms also collinear with N2A or N2B of the pyridine ring [N1A-Re1A-N2A = 177.3(3)º and N1B-Re1B-N2B = 178.2(2)°]. The equatorial plane is defined by the four bromo atoms and the rhenium(II) ion is slightly shifted from this mean plane by 0.146 (Re1A) and 0.144 Å (Re1B) Å towards the NO group.

Besides the anion-cation electrostatic interaction in **1**, there is a double hydrogen bond between the carboxylic groups [O···O distances of 2.560(5) and 2.690(5) Å] which connects the [Re(NO)Br_4(Hnic)]$^-$ units into pairs, the distance between the rhenium(II) ions being 12.146(7) Å (see Figure 2). π-type interactions between the pyridyl rings of adjacent supramolecular dimers lead to rectangular tetrameric units with a Re···Re separation through the diagonals of 14.076(7) Å.

Dalton Transactions Accepted Manuscript

[Re(NO)Br_4(μ-nic)Ni(dmphen)$_2$]·CH_3CN (2) and [Re(NO)Br_4(μ-pyc)Co(dmphen)$_2$]·MeOH (3). **2** and **3** are isostructural compounds and their structure is made up by neutral heterodinuclear units of [Re(NO)Br_4(μ-nic)M(dmphen)$_2$] [M = Ni (**2**), Co (**3**)] [Figures 3 (**2**) and S1 (**3**)] and half solvent molecule [MeCN (**2**) and MeOH (**3**)] of crystallization. Each unit contains Re(II) and M(II) metal ions which are bridged by one nicotinato group which adopts a didentate(carboxylate)/monodentate(pyridyl-nitrogen) coordination mode. The coordinated [Re(NO)Br_4(nic)] block in **2** and **3** is almost unchanged with respect to the [Re(NO)Br_4(Hnic)]$^-$ unit in **1** except for the deprotonation of the Hnic ligand upon its coordination to M(II). The rhenium(II) ion is surrounded by four bromo atoms, the NO group and the pyridine-nitrogen atom of nicotinate in a somewhat distorted octahedral geometry. The four set of Br atoms build the equatorial plane, the rhenium atom being shifted from this mean plane by 0.148 (**2**) and 0.143 Å (**3**) towards the NO group. The geometry of the $[ReNO]^{3+}$ core is unchanged, being pratically lineal [Re–N–O angles of 177.2(5) (**2**) and 176.0(9) Å (**3**)]. The Re–Br distances cover the range 2.5076(7) – 2.5266(7) Å, values which compare well with those found in **1**. Each M(II) ion is tris-chelated with two nicotinate–oxygen atoms and four nitrogen atoms from two didentate dmphen ligands building a distorted octahedral environment. The carboxylato group is coordinated in an assymetric fashion, with a short M–O distance [2.086(3) (**2**) and 2.093(5) Å (**3**)] and a longer one [2.305(3) (**2**) and 2.426(5) Å (**3**)]. The values of the M–N bond lengths vary in the range 2.065(3) – 2.124(4) for **2**, and 2.103(4) – 2.154(6) for **3**. The dmphen ligands are quite planar, the dihedral angle between them being 66.65 (**2**) and 66.64° (**3**).

The arrangement of the heterobimetallic units in the unit cell are shown in Figures 4 (**2**) and S2 (**3**). The shortest intermolecular Re···Ni and Re···Co distances are 7.3680(8) and 7.2706(10) Å respectively (red broken lines in Figures 4 and S2), values which are shorter than the intramolecular Re···M separations [7.8736(8) (**2**) and 7.9632(10) Å (**3**)].

[Re(NO)Br_4(μ-nic)Mn(dmphen)(H_2O)$_2$]·dmphen (4). The structure of **4** consists of neutral heterometallic [Re(NO)Br_4(μ-nic)Mn(dmphen)(H_2O)$_2$] units (Figure 5) and one co-crystallized dmphen molecule. As in **2** and **3**, the two metal ions in **4** are connected by a didentate [towards the Mn(II)]/monodentate [towards the Re(II)] nicotinate bridge, the intradimer Re···Mn distance being 7.7600(6) Å. The rhenium environment in **4** also remains almost unmodified (respect to that in **1**) upon formation of the heteropolynuclear species, with a Re–Br average distance and a Re–N–O angle of 2.5206(5) Å and 178.3(4)°, respectively. Each manganese(II) ion in **4** atom is six-coordinate being surrounded by two nitrogen atoms from a chelating dmphen molecule, and four oxygen atoms, two from water molecules and the other two belonging to the carboxylate of the nicotinate bridge. The equatorial plane of the distorted octahedral environment of the manganese(II) ion is defined by the N3O2O1WO2W set of atoms with the metal ion being shifted by 0.158 Å from this mean plane towards the N4 atom. The reduced bite of the chelating nicotinate ligand [57.30(9)° for O2–Mn–O3] is the main cause of the distortion of the manganese environment, as in **2** and **3**. The carboxylato group is again coordinated in an

Dalton Transactions Accepted Manuscript

assymetric fashion, with a short Mn–O2 distance of 2.201(3) Å and a longer Mn-O3 distance of 2.369(2) Å.

Besides an extended π stacking between the aromatic rings at the rhenium and manganese coordination spheres, the dmphen of crystallization and the pyridine rings of different units, short through space Br···Br contacts are present in the structure (Figure 6). The shortest bromo-bromo distance is 4.0269(5) Å [Br1···Br1^{i}; symmetry code: (i) = -*x*, 1-*y*, -*z*]. The coordinated dmphen molecules are arranged in a quasi parallel configuration respect to the uncoordinated ones. The dihedral angle between their mean planes of only 4.45(7)º and interplanar distances in the range of 3.640(2) - 3.746(2) Å. π-π staking interactions between free dmphen molecules [dmphen – dmphen^{ii}; (ii) = 1-*x*, -*y*,-*z*)] with an interplanar separation of 3.536(2) Å are also involved. Hydrogen bonds between water molecule O1W and the nitrogen atoms of the free dmphem molecule (N5 and N6) contribute to the stabilization of the structure (O-N distances 2.847(4) and 2.794(4) Å respectively).

[Re(NO)Br$_4$(μ-nic)Cu(bipy)$_2$] (5). The structure of complex **5** consists of neutral heterobimetallic [Re(NO)Br$_4$(μ-nic)Cu(bipy)$_2$] units where the Re(II) and Cu(II) metal ions are bridged by one nicotinate ligand as shown in Figure 7. The nicotinate ligand in **5** adopts the same bidentate [towards the Cu(II)]/monodentate [towards the Re(II)] bridging mode observed in **2**-**4** but it is more distorted, the intramolecular Re···Cu distance [8.2148(7) Å] being significantly longer than in the previous compounds. The great asymmetry of the chelate carboxylate at the copper(II) ion [1.962(3) and 2.821(3) Å for Cu1-O2 and Cu1-O3, respectively] account for this feature. The value of the longer copper-to-oxygen bond remains within the range reported for axial elongated Cu(II)-O bonds (2.22 to 2.89 Å).[20] The coordination sphere of the copper(II) ion in **5** is completed by four nitrogen atoms from two chelating bipy molecules, forming a highly distorted octahedron whose equatorial plane is defined by the O2N3N4N6 set of atoms. The Cu-N distances are in the range found for similar environments,[21] the average value being 2.051(4) Å. Both bipy ligands are planar and the dihedral angle between them is 72.47(9)°. Again, the Re(II) building block in **5** remains unchanged respect those in **2**-**4** with values of the average Re-Br bonds and Re1-N1-O1 angles of 2.5203(6) Å and177.9(5)°. Although the N-O distance in the nitrosyl group in **5** is larger than those found in **1**–**4,** due in part to the slight disorder of this group, it is similar to the distance found in other structures.[22] Finally, a view of the packing in **5** (Figure 8) shows the lack of significant through space bromo-bromo contacts (shortest Br···Br separation of 6.152(1) Å, [Br2···Br3^{ii}; symmetry code: (ii) = *x*, 0.5-*y*, 0.5+*z*]).

Magnetic Properties of 1-5 and 5'

Compound 1.

The octahedral ligand field for 5*d* metal ions is always strong and so, the d^5 electronic configuration of the Re(II) ion presents a low-spin ground term, $^2T_2$ (t_2^5). This orbitally

Dalton Transactions Accepted Manuscript

degenerated $^2T_2$ term in the case of **1** is splitted by the tetragonal ligand field and the spin-orbit coupling (SOC) such as shown in Figure 9. SOC splits the $^2T_2$ term into the doublet *E"* and the quadruplet *G'* (considering the double group, O'), being the doublet the ground state for $\lambda < 0$. In the absence of SOC, the tetragonal distortion (considering the C_{4v} point-group) splits the $^2T_2$ term into an orbital singlet, $^2B_2$, and an orbital doublet, ^2E, separated by an energy gap, Δ, which is defined as positive if the singlet is the lowest. Because of the strong spin-orbit coupling and ligand-field operating in the 5*d* metal ions, both perturbations must be taken into account simultaneously [eqn (1)].[1]

$$\hat{H} = \kappa\lambda\hat{L}\hat{S} + \hat{V}_{tetrag} \quad (1)$$

For any value of Δ (positive or negative), the ground state is always the doublet *E"* which is separated of the first excited state by more than $|\lambda|$ in energy. Due to the strong SOC ($\lambda \approx$ -2000 cm^{-1}), it can be assumed that this ground Kramers doublet is the only populated state in the whole temperature range. In this respect, we have previously shown that the magnetic susceptibility can be described by eqn (2).

$$\chi_u = \frac{N\beta^2 g_u^2}{4kT} + \chi_{TIP}^u \qquad \chi_M = \frac{\chi_\parallel + 2\chi_\perp}{3} \qquad (2a)$$

Being u = $\parallel$ or $\perp$ and χ_{TIP}^u the temperature-independent paramagnetism (TIP). The values of $g_\parallel$ and $g_\perp$ as well as those of $\chi_{TIP}^\parallel$ and $\chi_{TIP}^\perp$ are given by eqns (2b-2e)

$$g_\parallel = \frac{2(\kappa+1-a^2)}{(1+a^2)} \qquad (2b)$$

$$g_\perp = \frac{2\kappa a\sqrt{2}-a^2}{(1+a^2)} \qquad (2c)$$

$$\chi_{TIP}^\parallel = -\frac{2N\beta^2(\kappa+1-ab)}{\kappa\lambda(1+a^2)(1+b^2)Z} \qquad (2d)$$

$$\chi_{TIP}^\perp = -\frac{2N\beta^2}{\kappa\lambda}\left\{\frac{[\kappa(a+b)-ab\sqrt{2}]^2}{2Z(1+a^2)(1+b^2)} - \frac{(\sqrt{2}-\kappa a)^2}{(1+a^2)(v-1.5-Z)}\right\} \qquad (2e)$$

where $a = \frac{1}{\sqrt{2}}(v + 0.5 - Z)$, $b = \frac{1}{\sqrt{2}}(v + 0.5 + Z)$, $Z = \sqrt{v^2 + v + 2.25}$ and $v = \frac{\Delta}{\kappa\lambda}$

As one can see, the powdered experimental thermal dependence of the $\chi_M T$ product is expected to follow a straight line, $\chi_M T = A + BT$, being *A* the Curie constant, $\frac{N\beta^2 g_{av}^2}{4k}$, and *B* the average temperature-independent paramagnetism, χ_{av}^{TIP}.

Dalton Transactions Accepted Manuscript

Because of the large correlation existing between diamagnetism, χ_{dia}, and χ_{TIP}, the experimental magnetic susceptibility data obtained for **1** were carefully corrected for the diamagnetism of the constituent atoms and holder sample (see Physical Techniques).

The magnetic properties of **1** under the form of $\chi_M T$ *versus T* plot [χ_M is the magnetic susceptibility per one Re(II) ion] are shown in Figure 10. As predicted, a straight line is observed for this compound. The slight decrease at low temperatures can be attributed to very weak intermolecular antiferromagnetic interactions. Although there are two crystallographically non-equivalent $[Re(NO)Br_4(Hnic)]^-$ units in **1**, they are structurally quite similar, in particular the coordination geometry around the rhenium atom (see Table 2) and so, the same magnetic behaviour was assumed for them.

From eqn (2) and adding a Weiss constant, θ (in the form $T - \theta$), to take into account these intermolecular magnetic interactions, and using average values for *g* and χ_{TIP} ($g_{av}^2 = \frac{g_{\parallel}^2+2g_{\perp}^2}{3}$ and $\chi_{av}^{TIP} = \frac{\chi_{\parallel}^{TIP}+2\chi_{\perp}^{TIP}}{3}$), in order to avoid overparametrization, the experimental $\chi_M T$ data were successfully reproduced. Best-fit parameters are: g_{av} = 2.04(1) and χ_{av}^{TIP}= 140(5) x 10^{-6} cm^3 mol^{-1} and θ = -0.16 K. From these values and using eqns (2b-2e) we can estimate *k* = 0.65 and ν = -1.88 (for instance λ = -1850 cm^{-1} and Δ = 2260 cm^{-1}). Similar values were observed for other related nitrosyl Re(II) complexes. The value of *k* = 0.65 is indicative of a significant Re-ligand covalence.The value of Δ (axial distortion) is positive in sign, indicating that the orbital singlet, $^2B_2$, is lower than the doublet, ^2E, (Figure 9). The positive sign is in agreement with the electronic configuration expected for a tetragonal nitrosyl Re(II) complex.[15] Figure 11 shows a typical arrangement of the 5*d* metal orbitals (the Re-N-O bond defines the z-axis). The $d_{x^2-y^2}$ and d_{z^2} interact with the σ-donor ligand orbitals, increasing that their energy, whereas the d_{xz} and d_{yz} orbitals interact with the acceptor π^*_{NO} orbitals and their energies decrease. The d_{xy} orbital is relatively unperturbed.

In order to confirm the sign of the Δ parameter, we have studied the corresponding EPR spectra (see Figure 12). This spectrum clearly shows the existence of a spin doublet with an axial symmetry characterised by $g_{\parallel} < g_{\perp}$ [23] ($g_{\perp} \approx 2.32$ and $g_{\parallel} \approx 1.40$, $g_{av} \approx 2.05$) in agreement with a positve Δ value [see eqns (2b) and (2c)]. The sextet signal corresponds to the interaction of the unpaired electron with the nuclear spins of ^{185}Re and ^{187}Re with *I* = 5/2. The value of the hyperfine coupling parameter, *A* ≈ 400 G, is indicative of a relatively important delocalization of the unpaired electron towards the ligands, in agreement with the value orbital reduction parameter (*k* = 0.65).[24] Finally, the very weak intermolecular magnetic interactions must be attributed to the Br···Br contacts. In fact, the shortest Br···Br distance (3.84 Å) in **1** is slightly shorter than the Van der Waals one (*ca* 3.90 Å).[3c, 25]

Compounds 2 – 5 and 5'.

The magnetic properties of the compounds **2** – **5** and **5'** under the form of $\chi_M T$ *versus T* plot [χ_M

Dalton Transactions Accepted Manuscript

being the magnetic susceptibility per $Re^{II}M^{II}$ heterobimetallic unit] are shown in Figures 13 (**2**), S3 (**3**), S4 (**4**) and 14 (**5** and **5'**). The shape of these curves are qualitatively similar: a quasi Curie law behaviour in the high temperature domain followed by a smooth decrease at low temperature. At room temperature, the values of $\chi_M T$ are 4.25 (**2**), 2.65 (**3**), 5.45 (**4**), 2.00 (**5**) and 1.90 $cm^3\ mol^{-1}\ K$ (**5'**). They are as expected for magnetically non-interacting $Re^{II}M^{II}$ pairs [M **=** Ni (**2**), Co (**3**), Mn (**4**) and Cu (**5** and **5'**)]. The decrease of $\chi_M T$ suggests the presence of weak antiferromagnetic interactions M(II)-Re(II) and/or the zero-field splitting effects. Although the structures of **5'** is unknown, it is most likely a heterodinuclear compound as in **5** on the basis of the elemental analysis, analogy of the infrared absorptions of the nicotinato ligand and strong similarity of their magnetic curves.

Having these features in mind, the analysis of their magnetic data was performed through the Hamiltonian of eqn (3)

$$\hat{H} = -J\hat{S}_{Re}\cdot\hat{S}_M + D_M\left[\hat{S}^2_{ZM} - \frac{1}{3}S_M(S_M+1)\right] + \beta(g_{Re}\hat{S}_{Re} + g_M\hat{S}_M)\cdot H \qquad (3)$$

where J_{ReM} is the intradinuclear exchange coupling parameter, D_M is the local zero-field splitting of the M(II) ions with S > 1/2 (M = Mn, Co and Ni). The last term accounts for the Zeeman effects of the two metal ions and here, in order to avoid overparametrization, we have assumed that $g_x = g_y = g_z = g$ for both metal ions. Moreover, due to the $[Re(NO)Br_4(nic)]$ block is almost unchanged upon coordination to M(II), we have kept constant g_{Re} = 2.04 and $\chi_{(Re)TIP} \approx 140 \times 10^{-6}$ $cm^3\ mol^{-1}$ (values corresponding to those observed for **1**) in the fitting process. Least-squares fit of the magnetic data of **2** - **5** and **5'** using matrix-diagonalization techniques through the VPMAG program[26] provided the parameters listed in Table 6. A satisfactory match between the magnetic data and the calculated curves is obtained for all compounds in the whole temperature range investigated. In the case of **4** (M = Mn), we used a value of D_{Mn} = 0 because of the large isotropic character of the high spin six-coordinate Mn(II) ion.

It should be noted that the spin-Hamiltonian formalism of eqn (3) is applicable only to metal ions with non-degenerated orbital ground terms, that is, spin-only. This condition is satisfied by square pyramidal Cu(II) complexes, $^2B_1$, (**5** and **5'**), octahedral manganese(II), $^6A_{1g}$ (**4**) and nickel(II), $^3A_{2g}$ (**2**), but not by octahedral cobalt(II) (**3**) which has an orbital degenerated ground state, $^4T_{1g}$. Actually, the orbital contribution to the $\chi_M T$ value is very small due to the highly distorted environment of the Co(II) ions in **3**. The crystal field component of lower symmetry splits the T_1 term giving an orbital non-degenerate ground term, which can be considered the only populated state in all the temperature range investigated and that it is further split by second-order spin-orbit coupling (zero-field splitting). Under this assumption, we have studied the compound **3** by means of the spin Hamiltonian of eq (3). Nevertheless, we have also analyzed its magnetic data through the Hamiltonian of eqn (4), which is a bit more complicate given the presence of the orbital degenerate $^4T_{1g}$ ground term of the high spin six-coordinate Co(II) in **3**.[27a]

$$\hat{H} = -J\hat{S}_{Re}\hat{S}_{Co} - \alpha\lambda_{Co}\hat{S}_{Co}\hat{L}_{Co} + \Delta_{Co}\left[\hat{L}^2_{ZCo} - \frac{1}{3}L_{Co}(L_{Co}+1)\right] + \beta\left(g_{Re}\hat{S}_{Re} + g_e\hat{S}_{Co} + \alpha\hat{L}_{Co}\right)H \quad (4)$$

The first term corresponds to the isotropic exchange coupling between the Re^{II} and Co^{II} local

Dalton Transactions Accepted Manuscript

spins. The second term takes into account the spin-orbit coupling between the S = 3/2 spin and the L = 1 effective angular moment for the $^4T_{1g}$ ground term of Co^{II}. In this term, λ is the spin-orbit coupling parameter and $\alpha = \kappa A$ where κ is the orbital reduction factor and A describes the strength of the crystal field (A = 3/2 and 1 for the weak and strong crystal field limits, respectively). In the third term, Δ_{Co} represents the energy gap between the ^4E and ^4A levels originated from the splitting of the $^4T_{1g}$ ground state in octahedral geometry (axial distortion).[27a] Finally, the last term accounts for the Zeeman effects on the two metal ions, being g_e the g factor for the free electron.

Least-squares fit of the magnetic data of **3** through eqn (4) using matrix diagonalization techniques from the magnetic package VPMAG[26] led to the following set of parameters: J_{ReCo} = -0.52(2) cm^{-1}, α = 1.24(1), λ_{Co} = −110(2) cm^{-1}, Δ_{Co} = 740(10) cm^{-1}. As above, we kept constant g_{Re} = 2.04 and $\chi_{(Re)TIP} \approx 140 \times 10^{-6}$ cm^3 mol^{-1} during the fit process. A satisfactory match between the magnetic data and the calculated curve is achieved in the whole temperature range. These values are very close to other observed for similar distorted six-coordinate Co(II) ions.[27] The large value for Δ_{Co} indicates a very large distortion of the octahedral surrounding caused by the chelating dmphen and it justifies both the use of the Hamiltonian of eqn (3) and the high value of the zfs of the Co(II) ion (D_{Co} = 22 cm^{-1}).[27d] The values of the J_{ReCo} obtained through the two models are similar.

Recently, some of us have studied the magnetic properties of a family of heterodinuclear complexes of Re(IV) with divalent metal ions, [X_5Re(μ-2-pyzc)M(dmphen)$_2$], X = Cl^- or Br^-, M = Ni(II) or Co(II), 2-pyzc = 2-pyrazinecarboxylate and dmphen = 2,9-dimethyl-1,10-phenantroline.[28] The analysis of the exchange magnetic interaction between Re(IV)-M(II) through the 2-pyzc bridging ligand showed the occurrence of intramolecular ferromagnetic interactions ($J \approx$ 0.7 - 2.1 cm^{-1}). Similar ferromagnetic exchange interactions were observed when using the oxalato anion as bridging ligand ($J \approx$ 10 - 12 cm^{-1}).[29] Although the corresponding carboxylato bridging ligands are different in all these cases, it is important to note that in the case of Re(IV) the magnetic interaction is ferromagnetic in nature, while for the Re(II) complexes weak antiferromagnetic interactions occur.

In order to understand this difference, it is important to take into account the different magnetic orbitals on each metal centre. Re(IV) has three unpaired electrons in the d_{xz}, d_{yz} and d_{xy} orbitals (see Figure 11 but placing therein only three unpaired electrons instead of the five electrons which are shown). The presence of d_{xz} or d_{yz} magnetic orbitals allows an important spin delocalization on the bridge [see Scheme 1a with Re(IV) instead of Re(II)]. The orthogonality between this spin density on the bridge and the magnetic orbital on the other divalent metal ion, Ni(II) or Co(II), takes account for the observed ferromagnetic interaction. In the case of the Re(II) derivatives (compounds **1** - **5**), the Re(II) ion has only one unpaired electron in the d_{xy} orbital (due to $\Delta > 0$) as shown in Figure 11. As it is shown in Scheme 1b, the symmetry of this magnetic orbital precludes any spin delocalization on the orbitals of the bridging ligand. In this respect, the weak antiferromagnetic interaction observed for **2** – **5** and **5'** should be attributed to interdinuclear magnetic interactions rather than an intradinuclear pathway through the nicotinato

Dalton Transactions Accepted Manuscript

bridge.

A detailed inspection of the structures of **2** – **5** reveals the occurrence of large through space Br···Br distances [values greater than 5.5 Å which much larger than the van der Waals ones (*ca* 3.9 Å)] between adjacent $Re^{II}M^{II}$ heterobimetallic units for **2**, **3** and **5**, discarding thus any significant interdinuclear magnetic interaction through this pathway in these compounds. Nevertheless, significant short Br···Br contacts (*ca* 4.03 Å) occur In the case of **4**. Moreover, there are π–π contacts between the aromatic rings of the dmphen molecules (several C---C distances smaller than 3.5 Å), in **2** – **5** suggesting a possible pathway for interdinuclear magnetic interactions. In fact, we can fit the experimental magnetic susceptibility data neglecting any intradinuclear Re(II)-M(II) magnetic interaction (that is J = 0) and adding a θ interdimer Weiss parameter (in the form $T - \theta$). The best-fit parameters are listed in Table 6.

Finally, it is interesting to note that Palii *et al*. have reported the first and unique study about the magnetic interaction between Re(II) and other paramagnetic metal centers.[30] They have investigated the magnetic interaction of Re(II)-(μ-CN)-Mn(II) in a Re_4Mn_4 cubane-type octanuclear complex, observing relatively large J values mediated by the cyanido bridge (J_{ReMn} *ca* -20 cm^{-1}). In this case, the Re(II) presents such a distorted octahedral surrounding that a negative value for Δ parameter ($\Delta < 0$) is involved. So, in this case the magnetic orbital of the Re(II) ion is d_{xz} (and/or d_{yz}, see Figure 11) whose symmetry allows a very large delocalization on the cyano bridge (see Scheme 1c). The antiferromagnetic interaction [in contrast to the ferromagnetic one observed for Ni(II) and Co(II) in compounds **2** and **3**] has to be attributed to the existence of five magnetic orbitals on the Mn(II) ion, one of them being able to overlap with that of the Re(II) (as shown in Scheme 1c), leading to a global antiferromagnetic exchange interaction.

Conclusions

In the present work we have prepared and characterized the $[Re(NO)Br_4(Hnic)]^-$ anionic complex. In a second step, this complex was used as ligand towards partially blocked M(II) units, where M is a 3d paramagnetic cation. Heterobimetallic Re(II)-M(II) complexes were isolated upon deprotonation of the carboxylic group. The full characterization of the species demonstrated the capability of 3-pyridinecarboxylate to act as bridging ligand. Compunds **2** – **5** are the first examples of heterodinuclear complexes containing Re(II).

The monomer $NBu_4[Re(NO)Br_4(Hpyc)]$ behaves as a quasi magnetically isolated spin doublet with very weak antiferromagnetic interactions through space Br···Br contacts. Its magnetic susceptibility data were successfully modeled through a deep analysis of the influence of the ligand field, spin-orbit coupling, tetragonal distortion and covalence effects as variable parameters. The heterobimetalic complexes exhibit weak antiferromagnetic interactions, most likely mediated by π-π type interactions between the peripheral ligands. Only in the case of the Mn compound**,** short through space Br···Br contacts were involved in the exchange coupling.

Acknowledgements

Dalton Transactions Accepted Manuscript

Financial support from PEDECIBA (Uruguay), CSIC (Uruguay, Programa de Apoyo a Grupos de Investigación and Proyecto de Iniciación 510) and Ministerio Español de Ciencia e Innovación (Project CTQ2014-44844P) is gratefully acknowledged. This work has also been partially supported by MINECO under The National Program of Materials (MAT2013-46649-C4-4-P), The Consolider-Ingenio 2010 Program (MALTA CSD2007-00045), and by the EU-FEDER funds. M.P. acknowledges CAP-UdelaR (Uruguay) for a grant.

References

1. M. Pacheco, A. Cuevas, J. González-Platas, R. Faccio, F. Lloret, M. Julve and C. Kremer, *Dalton Trans.*, 2013, **42**, 15361.

2. (a) C. E. Uzelmeier, S. L. Bartley, M. Fourmigué, R. Rogers, G. Grandinetti and K. R. Dunbar, *Inorg. Chem.*, 1998, **37**, 6706; (b) E. J. Schelter, J. K. Bera, J. Bacsa, J. R. Galán-Mascarós and K. R. Dunbar, *Inorg. Chem.*, 2003, **42**, 4256; (c) K. R. Dunbar, E. J. Schelter, B. S. Tsukerblat, S. M. Ostrovsky, V. Y. Mirovitsky and A. V. Palii, *Polyhedron*, 2003, **22**, 2545; (d) K. R. Dunbar, E. J. Schelter, A. V. Palii, S. M. Ostrovsky, V. Y. Mirovitskii, J. M. Hudson, M. A. Omary, S. I. Klokishner and B. S. Tsukerblat, *J. Phys. Chem. A*, 2003, **107**, 11102.

3. (a) R. González, A. Acosta, R. Chiozzone, C. Kremer, D. Armentano, G. De Munno, M. Julve, F. Lloret and J. Faus, *Inorg. Chem.*, 2012, **51**, 5737; (b) A. Cuevas, C. Kremer, L. Suescun, S. Russi, A. W. Mombrú, F. Lloret, M. Julve and J. Faus, *Dalton Trans.*, 2007, 5305; (c) A. Cuevas, C. Kremer, M. Hummert, H. Schumann, F. Lloret, M. Julve and J. Faus, *Dalton Trans.*, 2007, 342; (d) J. Martínez-Lillo, J. Faus, F. Lloret and M. Julve, *Coord. Chem. Rev.*, 2014, http://dx.doi.org/10.1016/j.ccr.2014.11.007; (e) J. Martínez-Lillo, J. Kong, W. P. Barros, J. Faus, M. Julve and E. K. Brechin, *Chem. Commun.*, 2014, **50**, 5840.

4. (a) J. Mrozinski, A. Kochel and T. Lis, *J. Mol. Struct.*, 2002, **610**, 53; (b) J. Mrozinski, A. Kochel and T. Lis, *J. Mol. Struct.*, 2002, **641**, 109; (c) A. Tomkiewicz, J. Mrozinski, I. Brüdgam and H. Hartl, *Eur. J. Inorg. Chem.*, 2005, 1787; (d) B. Machura, A. Jankowska, R. Kruszynski, J. Klak and J. Mrozinski, *Polyhedron*, 2006, **25**, 1348.

5. (a) T. D. Harris, M. V. Bennett, R. Clérac and J. R. Long, *J. Am. Chem. Soc.*, 2010, **132**, 3980; (b) T. D. Harris, C. Coulon, R. Clérac and J. R. Long, *J. Am. Chem. Soc.*, 2011, **133**, 123; (c) T. D. Harris, H. S. Soo, C. J. Chang and J. R. Long, *Inorg. Chim. Acta*, 2011, **369**, 82; (d) X. Feng, T. D. Harris and J. R. Long, *Chem. Sci.*, 2011, **2**, 1688; (e) X. Feng, J. Liu, T. D. Harris, S. Hill and J. R. Long, *J. Am. Chem. Soc.*, 2012, **134**, 7521.

6. (a) I. Bhowmick, E. A. Hillard, P. Dechambenoit, C. Coulon, T. D. Harris and R. Clérac, *Chem. Commun.*, 2012, **48**, 9717; (b) I. Bhowmick, T. D. Harris, P. Dechambenoit, E. A. Hillard, C. Pichon, I.-R. Jeon and R. Clérac, *Sci. China: Chm.*, 2012, **55**, 1004; (c) K. S. Pedersen, M. Sigrist, M. A. Sørensen, A.-L. Barra, T. Weyhermüller, S. Piligkos, C. Aa. Thuesen, M. G. Vinum, H. Mutka, H. Weihe, R. Clérac and J. Bendix, *Angew. Chem. Int. Ed.*, 2014, **53**, 1351.

Dalton Transactions Accepted Manuscript

7. D. G. Samsonenko, C. Paulsen, E. Lhotel, V. S. Mironov and K. E. Vostrikova, *Inorg. Chem.*, 2014, **53**, 10217.

8. R. A. Coxsall, S. G. Harris, D. K. Henderson, S. Parsons, P. A. Tasker and R. E. P. Winpenny, *J. Chem. Soc., Dalton Trans.*, 2000, 2349.

9. (a) A. Earnshaw, *Introduction to Magnetochemistry*, Academic Press, London, 1968; (b) R. Boca, *Theoretical Foundations of Molecular Magnetism*, *Current Methods in Inorganic Chemistry*, Volume 1, Elsevier Science, 1999.

10. CrysAlisPro, Agilent Technologies, Version 1.171.35.19, (2011).

11. L. Palatinus and G. Chapuis. *J. Appl. Cryst.* **40**, 786 (2007).

12. G. M. Sheldrick, *Acta Crystallogr., Sect A: Fundam. Crystallogr.,* 2008, **64**, 112.

13. L. A. Spek. *Acta Crystallogr., Sect A: Fundam. Crystallogr.*, 1990, **46**, C-34.

14. O. V. Dolomanov, L. J. Bourhis, R. J. Gildea, J. A. K. Howard and H. Puschmann, *J. Appl. Cryst.,* 2009, **42**, 339.

15. B. Machura, *Coord. Chem. Rev.*, 2005, **249**, 2277.

16. K. Nakamoto, *Infrared and Raman Spectra of Inorganic and Coordination Compounds*, 6th edition, John Wiley & Sons, Inc., New Jersey, 2009.

17. G. Ciani, D. Giusto, M. Manassero and M. Sansoni. *J. Chem. Soc., Dalton Trans.*, 1975, 2156.

18. G. Ciani, D. Giusto, M. Manassero and M. Sansoni. *J. Chem. Soc., Dalton Trans.*, 1977, 798.

19. M. Pacheco, A. Cuevas. J. González-Platas and C. Kremer. *Commun. Inorg. Synth.*, 2014, **2**, 20.

20. B. J. Hathaway, in G. Wilkinson, R. D. Gillard and J. A. McCleverty (Eds.), *Comprehensive Coordination Chemistry*, vol. 5, Pergamon Press, New York, 1987, p. 603.

21. (a) W. D. Harrison and B. J. Hathaway, *Acta Crystallogr., Section B,* 1979, **35**, 2910; (b) J. Foley, S. Tyagi and B. J. Hathaway, *J. Chem. Soc., Dalton Trans*., 1984, 1.

22. (a) C. S. Pratt and J. A. Ibers, *Inorg. Chem.*, 1972, **11**, 2812; (b) V. G. Albano, A. Araneo, P. L. Bellon, G. Ciani and M. Manassero, *J. Organomet. Chem*., 1974, **67**, 413; (c) V. G. Albano, P. Bellon and M. Sansoni, *J. Chem. Soc. A*, 1971, 2420.

23. J. H. E. Griffit and J. Owen, *Proc. R. Soc. London, Ser. A*, 1954, **226**, 96.

24. (a) B. Machura, J. O. Dziegielewski, S. Michalik, T. J. Bartczak, R. Kruszynski and J. Kusz, *Polyhedron*, 2002, **21**, 2617; (b) S. R. Chowdhury, S. Dinda, S. Chakraborty, C. Simonnet, A. K. Mukherjee, K. I. Okamoto and R. Bhattacharyya, *Inorg. Chem. Commun.*, 2005, **8**, 61.

25. (a) R. González, R. Chiozzone, C. Kremer, F. Guerra, G. De Munno, F. Lloret, M. Julve and J. Faus, *Inorg. Chem.*, 2004, **43**, 3013; (b) J. Martínez-Lillo, D. Armentano, G. De Munno, M. Julve, F. Lloret and J. Faus, *Dalton Trans.*, 2013, **42**, 1687.

26. J. Cano, VPMAG program, Universitat de València, Spain, 2001.

27. (a) F. Lloret, M. Julve, J. Cano, C. Ruiz-García and E. Pardo, *Inorg. Chim. Acta*, 2008, **361**, 3432; (b) A. K. Sharma, F. Lloret and R. Mukherjee, *Inorg. Chem.*, 2007, **46**, 5128; (c) O. Fabelo, J. Pasan, F. Lloret, M. Julve and C. Ruiz-Pérez, *Inorg. Chem.*, 2008, **47**, 3568; J.

Dalton Transactions Accepted Manuscript

Vallejo, I. Castro, R. Ruiz-García, J. Cano, M. Julve, F. Lloret, G. De Munno, W. Wernsdorfer and E. Pardo, *J. Am. Chem. Soc.,* **2012**, *134*, 15704.

28. (a) A. Cuevas, C. Kremer, M. Hummert, H. Schumann, F. Lloret, M. Julve and J. Faus, *Dalton Trans.* 2007, 342; (b) L. Arizaga, R. González, D. Armentano, G. De Munno, M. A. Novak, F. Lloret, C. Kremer and R. Chiozzone, submitted.

29. (a) R. Chiozzone, R. González, C. Kremer, G. De Munno, D. Armentano, F. Lloret and J. Faus, *Inorg. Chem.*, 2003, **42,** 1064; (b) J. Martínez-Lillo, F. S. Delgado, C. Ruiz-Pérez, F. Lloret, M. Julve and J. Faus, *Inorg. Chem.*, 2007, **46**, 3523.

30. A. V. Palii, S. M. Ostrovsky, S. I. Klokishner, B. S. Tsukerblat, E. J. Schelter, A. V. Prosvirin and K. R. Dumbar, *Inorg. Chim. Acta*, 2007, **360**, 3915.

Dalton Transactions Accepted Manuscript

Table 1. Summary of the crystal data for compounds **1**-**5**[a]

	1	**2**	**3**	**4**	**5**
Chem. formula	$C_{22}H_{41}Br_4N_3O_3Re$	$C_{70}H_{59}Br_8N_{13}Ni_2O_6Re_2$	$C_{69}H_{60}Br_8Co_2N_{12}O_7Re_2$	$C_{34}H_{32}Br_4MnN_6O_5Re$	$C_{26}H_{20}Br_4CuN_6O_3Re$
M	901.42	2307.40	2298.83	1165.43	1033.86
Cryst. syst.	Triclinic	Monoclinic	Monoclinic	monoclinic	monoclinic
Space group	*P*-1	*P* 1 2_1/*n* 1	*P* 1 2_1/*n* 1	*P* 1 2_1/*c* 1	*P* 1 2_1/*c* 1
a/Å	11.8626(4)	11.74860(10)	11.7505(2)	10.96409(15)	11.61543(13)
b/Å	14.7096(5)	19.72731(14)	19.9118(3)	19.3015(3)	16.76550(16)
c/Å	20.6473(7)	18.11565(14)	18.0279(4)	18.0987(3)	16.03665(17)
α/deg	83.720(3)	90	90	90	90
β/deg	74.333(3)	108.2729(9)	107.768(2)	96.1198(13)	94.4673(10)
γ/deg	69.949(3)	90	90	90	90
V/Å^3	3258.2(2)	3986.91(6)	4016.86(15)	3808.28(10)	3113.47(6)
Z	4	2	2	4	4
D_c/Kg m^{-3}	1.838	1.922	1.901	2.033	2.206
crystal dim./mm^3	0.03 x 0.07 x 0.10	0.06 x 0.29 x 0.32	0.09 x 0.17 x 0.26	0.03 x 0.12 x 0.16	0.19 x 0.24 x 0.34
F(000)	1732	2208	2196	2232	1944
2θ range/º	6.40 – 133.19	6.82- 133.18	6.80 – 133.20	6.72 – 133.20	7.63 – 133.20
μ(Cu Kα)/cm^{-1}	13.239	11.474	14.043	14.141	14.668
refln./unique/obs.	22869/11247/9083	27246/7024/6768	15100/7086/6321	15095/ 6715/ 6057	11554/5489/5085
restraints/ref. param.	0/625	14/474	1/464	0/465	0/371
max/min $\Delta\rho$/ e A^{-3}	0.68/-0.73	1.33/-0.80	2.21/-1.09	0.57/-0.52	1.38/-1.24
R_{int}	0.0213	0.0213	0.0293	0.0184	0.0302
R^b	0.0316	0.0322	0.0450	0.0236	0.0330
$R_w{}^c$	0.0773	0.0851	0.1194	0.0575	0.0871
S^d	1.025	1.122	1.052	1.067	1.052

[a]Details in common: *T* = 20 °C, $I > 2\sigma(I)$. [b] $R = \frac{\Sigma||F_o|-|F_c||}{\Sigma|F_o|}$. [c] $R_w = \sqrt{\frac{\sum\left[w\left(F_o^2-F_c^2\right)^2\right]}{\sum\left[w\left(F_o^2\right)^2\right]}}$. [d]Goodness of fit: $S = \sqrt{\frac{\sum\left[w\left(F_o^2-F_c^2\right)^2\right]}{(N-P)}}$.

Dalton Transactions Accepted Manuscript

Table 2. Selected bond distances (Å) and bond angles (°) for **1**

Distances			
Re1A-N1A	1.743(6)	Re1B-N1B	1.738(5)
Re1A-N2A	2.226(4)	Re1B-N2B	2.228(4)
Re1A-Br1A	2.5255(9)	Re1B-Br1B	2.5227(9)
Re1A-Br2A	2.5073(9)	Re1B-Br2B	2.5171(8)
Re1A-Br3A	2.5137(10)	Re1B-Br3B	2.5104(7)
Re1A-Br4A	2.5253(9)	Re1B-Br4B	2.5175(7)
N1A-O1A	1.164(9)	N1B-O1B	1.167(8)
Angles			
Re1A-N1A-O1A	176.9(7)	Re1B-N1B-O1B	179.7(7)
N1A-Re1A-N2A	177.3(3)	N1B-Re1B-N2B	178.2(2)
Br1A-Re1A-Br3A	174.03(3)	Br1B-Re1B-Br3B	173.23(3)
Br2A-Re1A-Br4A	172.23(3)	Br2B-Re1B-Br4B	173.51(3)
N1A-Re1A-Br1A	91.7(2)	N1B-Re1B-Br1B	92.8(2)
N1A-Re1A-Br3A	94.3(2)	N1B-Re1B-Br3B	94.0(2)
N2A-Re1A-Br1A	86.49(12)	N2B-Re1B-Br1B	86.86(12)
N2A-Re1A-Br3A	87.55(12)	N2B-Re1B-Br3B	86.37(12)
O2A-C6A-O3A	123.9(5)	O2B-C6B-O3B	123.5(5)

Dalton Transactions Accepted Manuscript

Tabla 3. Selected bond distances (Å) and bond angles (°) for **2** (M = Ni) and **3** (M = Co)

Distances		
	2	**3**
Re1-N1	1.746(5)	1.732(7)
Re1-N2	2.225(3)	2.220(5)
Re1-Br1	2.5135(7)	2.5163(11)
Re1-Br2	2.5076(7)	2.5120(9)
Re1-Br3	2.5266(7)	2.5101(9)
Re1-Br4	2.5229(7)	2.5238(9)
N1-O1	1.173(8)	1.179(11)
M1-O2	2.086(3)	2.093(5)
M1-O3	2.305(3)	2.426(5)
M1-N3	2.124(4)	2.154(6)
M1-N4	2.083(4)	2.112(5)
M1-N5	2.065(3)	2.103(4)
M1-N6	2.082(3)	2.145(4)
Angles		
	2	**3**
Re1-N1-O1	177.2(5)	176.0(9)
N1-Re1-N2	177.9(2)	178.2(3)
Br1-Re1-Br3	172.37(3)	174.22(4)
Br2-Re1-Br4	174.09(3)	172.70(4)
N1-Re1-Br1	95.58(17)	92.3(3)
N1-Re1-Br3	92.05(17)	93.5(3)
N2-Re1-Br1	86.46(10)	87.88(11)
N2-Re1-Br3	85.92(10)	86.34(11)
O2-C6-O3	122.3(4)	122.4(6)
O2-M1-O3	59.86(11)	57.64(14)
N6-M1-O2	84.94(13)	83.40(17)
N3-M1-O3	76.92(13)	74.82(19)
N6-M1-N5	81.50(13)	79.78(16)
N3-M1-N4	79.77(14)	78.7(2)
N5-M1-N4	103.19(14)	105.48(19)

Dalton Transactions Accepted Manuscript

Table 4. Selected bond distances (Å) and bond angles (°) for **4**

Distances			
Re1-N1	1.824(4)	Mn1-O2	2.201(3)
Re1-N2	2.231(2)	Mn1-O3	2.369(2)
Re1-Br1	2.5226(5)	Mn1-O1W	2.182(2)
Re1-Br2	2.5243(5)	Mn1-O2W	2.194(3)
Re1-Br3	2.5129(5)	Mn1-N3	2.229(2)
Re1-Br4	2.5226(5)	Mn1-N4	2.248(3)
N1-O1	0.988(5)		
Angles			
Re1-N1-O1	178.3(4)	O2-C6-O3	121.3(3)
N1-Re1-N2	179.26(12)	O2-Mn1-O3	57.30(9)
Br1-Re1-Br3	171.73(2)	N3-Mn1-O1W	85.39(9)
Br2-Re1-Br4	174.76(2)	N4-Mn1-O2W	86.56(9)
N1-Re1-Br1	94.77(10)	N3-Mn1-N4	75.70(9)
N1-Re1-Br3	93.44(10)	O1W-Mn1-O2W	169.45(9)
N2-Re1-Br1	85.97(7)	N4-Mn1-O3	165.23(8)
N2-Re1-Br3	85.83(7)	N3-Mn1-O2	172.20(9)

Table 5. Selected bond distances (Å) and bond angles (°) for **5**

Distances			
Re1-N1	1.738(6)	Cu1-O2	1.962(3)
Re1-N2	2.215(3)	Cu1-O3	2.821(3)
Re1-Br1	2.5397(7)	Cu1-N3	2.040(4)
Re1-Br2	2.5114(7)	Cu1-N4	1.985(4)
Re1-Br3	2.5130(8)	Cu1-N5	2.182(3)
Re1-Br4	2.5171(5)	Cu1-N6	1.996(3)
N1-O1	1.175(8)		
Angles			
Re1-N1-O1	177.9(5)	O2-C6-O3	125.3(4)
N1-Re1-N2	178.9(2)	O2-Cu1-O3	51.67(12)
Br1-Re1-Br3	171.83(3)	N4-Cu1-O2	91.91(17)
Br2-Re1-Br4	174.93(2)	N6-Cu-O2	88.90(14)
N1-Re1-Br1	94.31(18)	N6-Cu-N5	78.78(13)
N1-Re1-Br3	93.71(18)	N3-Cu-N4	80.50(18)
N2-Re1-Br1	85.40(9)	N5-Cu-N4	102.77(15)
N2-Re1-Br3	86.55(9)		

Table 6. Best-fit parameters for **2**–**5** and **5'**

Compound	g_M	[a] D_M	[a] J (θ = 0)	[a] θ/K (J = 0)
2	2.22(1)	5.10(2)	-0.60(1)	-0.240(2)
3	2.38(2)	22.0(3)	-0.54(1)	-0.310(2)
4	2.00(1)	0.0	-0.45(1)	-0.341(2)
5	2.10(1)	--	-0.59(1)	-0.242(2)
5'	2.10(1)	--	-0.90(2)	-0.403(3)

[a] D_M and J values are given in cm^{-1}. [b] θ is a Curie-Weiss parameter (see text)

Dalton Transactions Accepted Manuscript

Dalton Transactions Accepted Manuscript

Chart 1. Coordination modes of nic ligand as a bridge: (left) 2.111; (middle) 2.011; (right) 3.111. The Harris notation is used to describe them (see ref.[8])

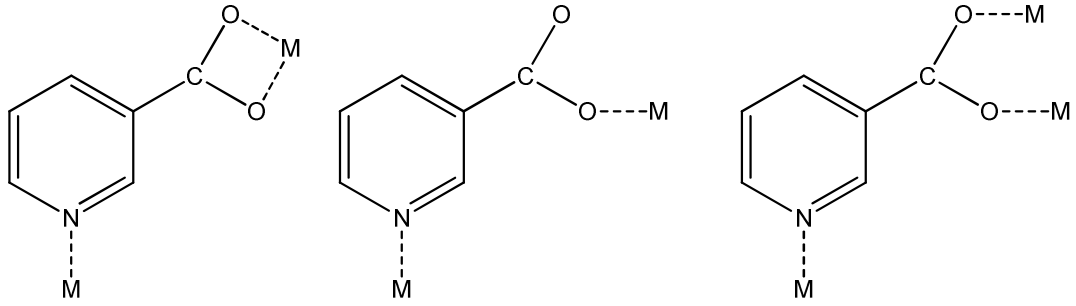

Figure 1. View of the anionic complex of **1** showing the atom numbering. Thermal ellipsoids are plotted at 30% probability level, and the hydrogen atoms were omitted for clarity.

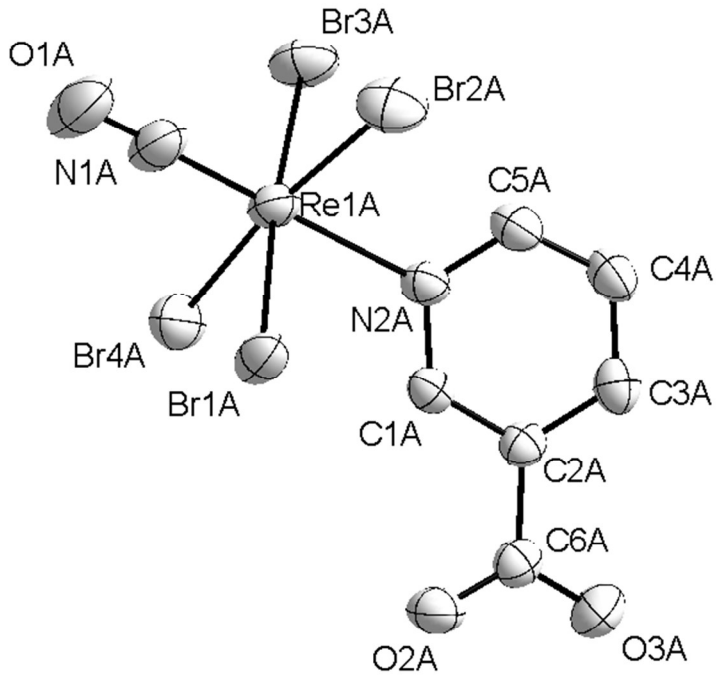

Dalton Transactions Accepted Manuscript

Figure 2. A projection view along the crystallographic *a* axis showing the supramolecular interactions **1**. The purple octahedron correspond to the coordination environment of the Re(II) ions and the dashed lines represent the hydrogen bonds connecting the anionic entities. Cations were omitted for clarity.

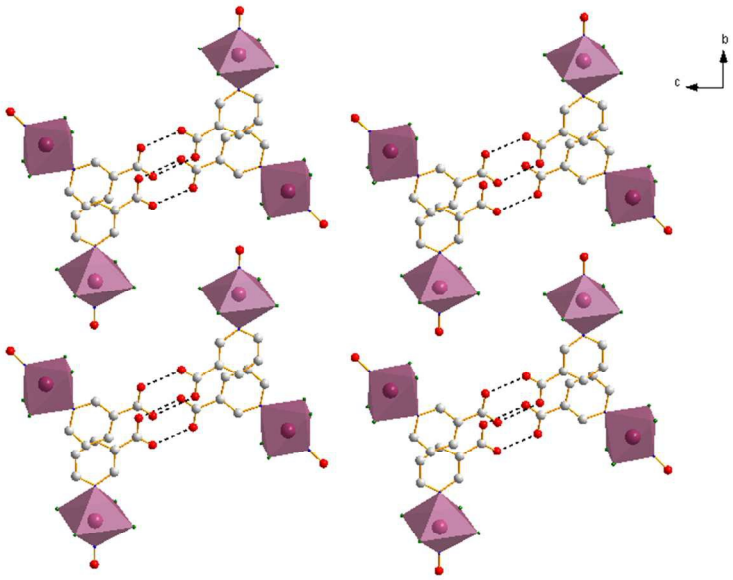

Figure 3. Perspective drawing of the $[Re(NO)Br_4(\mu\text{-nic})Ni(dmphen)_2]$ heterobimetallic unit of **2** showing the atom numbering. Thermal ellipsoids are plotted at 30% probability level, and the

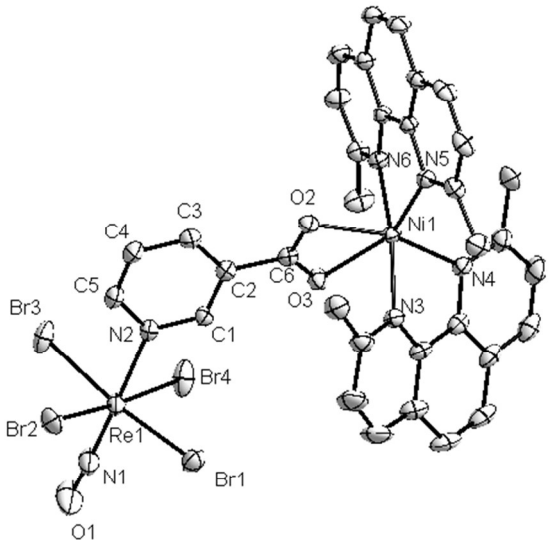

Dalton Transactions Accepted Manuscript

hydrogen atoms were omitted for clarity. The same atom numbering was adopted for **3**.

Figure 4. A view of the crystal packing of **2**. Purple and pale green octahedrons represent the coordination environment of the Re(II) and Ni(II) ions, respectively. The shortest Re···Ni distances are drawn as red broken lines.

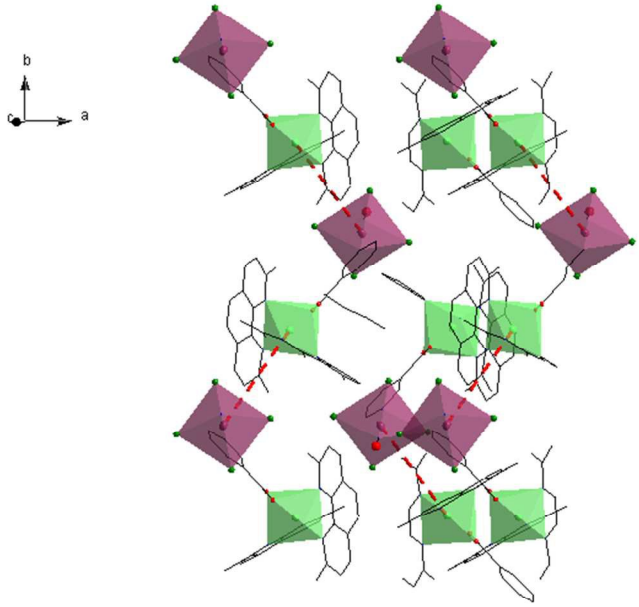

Figure 5. Perspective drawing of the heterobimetallic $[Re(NO)Br_4(\mu\text{-nic})Mn(dmphen)(H_2O)_2]$ unit of **4** showing the atom numbering. Thermal ellipsoids are plotted at 30% probability level, and the hydrogen atoms were omitted for clarity.

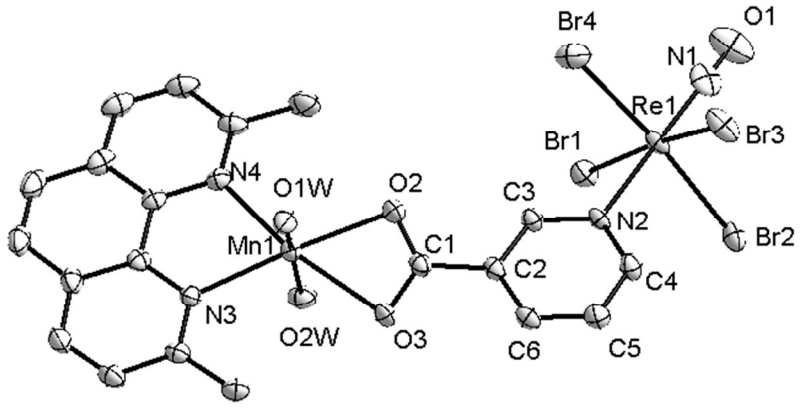

Dalton Transactions Accepted Manuscript

Figure 6. View of a fragment of the crystal packing in **4** showing the intermolecular Br···Br contacts (dashed red lines) connecting the heterobimetallic units. Color code: Re, purple; Br, dark green; Co, pink; N, blue; O, red; C, grey.

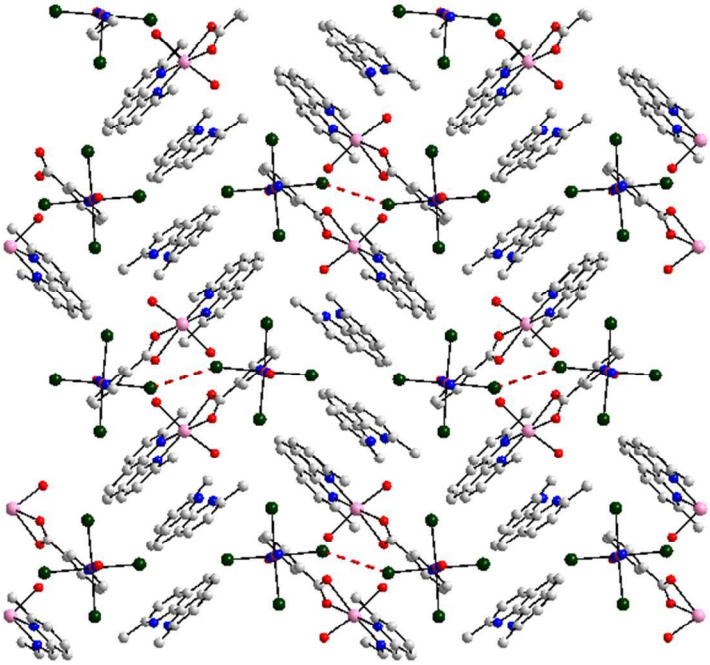

Dalton Transactions Accepted Manuscript

Figure 7 Perspective drawing of the $[Re(NO)Br_4(\mu\text{-nic})Cu(bipy)_2]$ heterobimetallic unit showing the atom numbering. Thermal ellipsoids are plotted at 30% probability level, and hydrogen atoms were omitted for clarity.

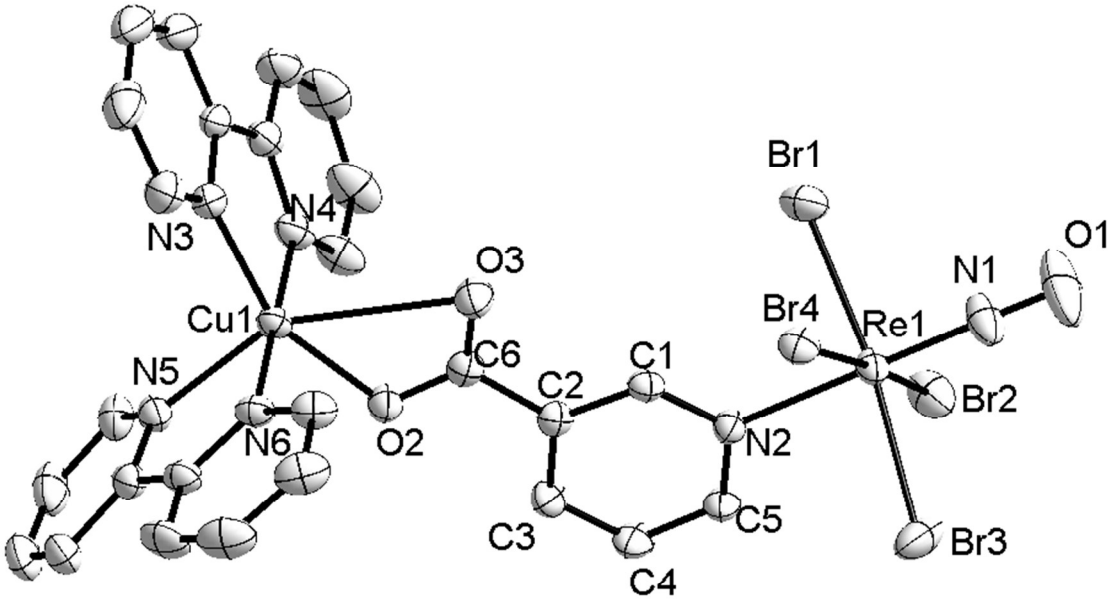

Dalton Transactions Accepted Manuscript

Figure 8 Partial view of the packing along the crystallographic *b* axis in **5**. Rhenium atoms are shown as purple octahedrons, and copper atoms as light blue ones. Hydrogen atoms have been omitted for clarity.

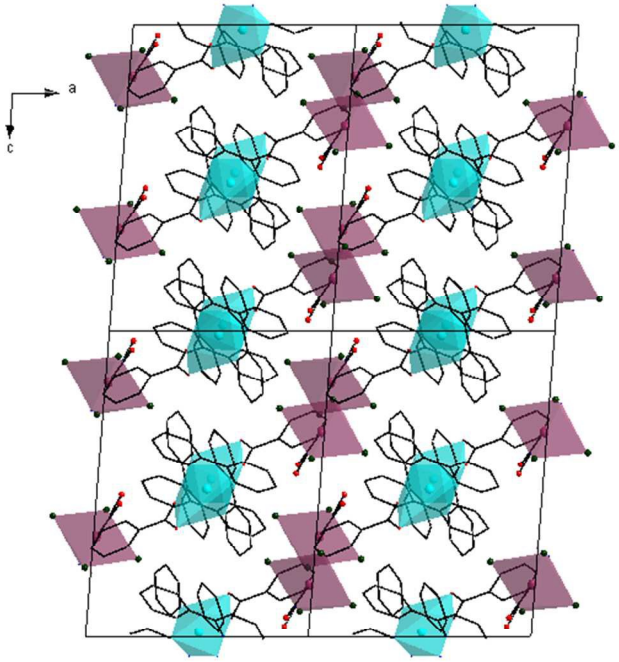

Dalton Transactions Accepted Manuscript

Figure 9. Splitting of the $^2T_{2g}$ term by spin-orbit coupling and a tetragonal distortion

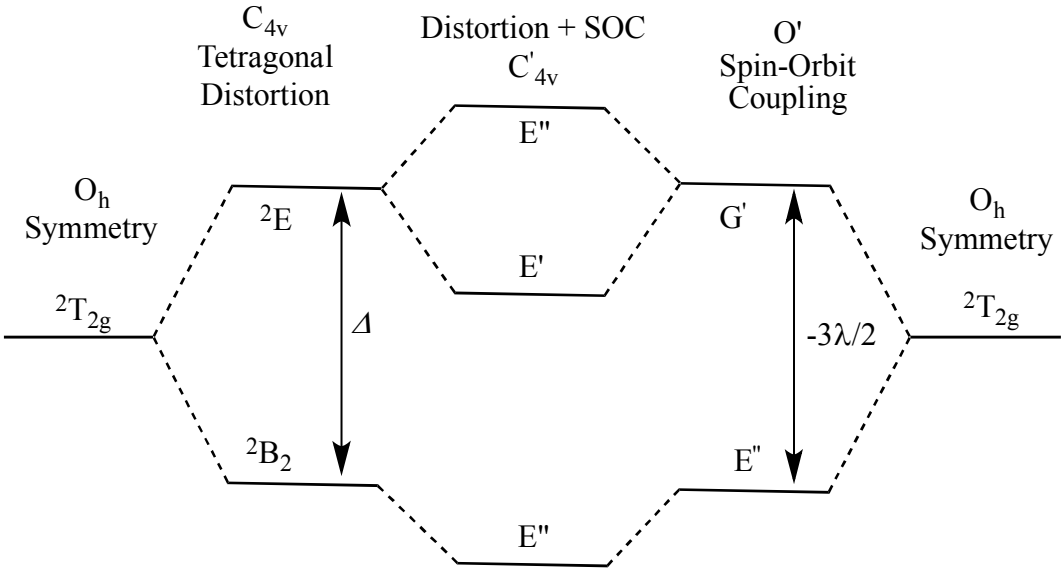

Figure 10. Thermal dependence of the $\chi_M T$ product for **1**: (o) experimental; (—) best-fit curve (see text).

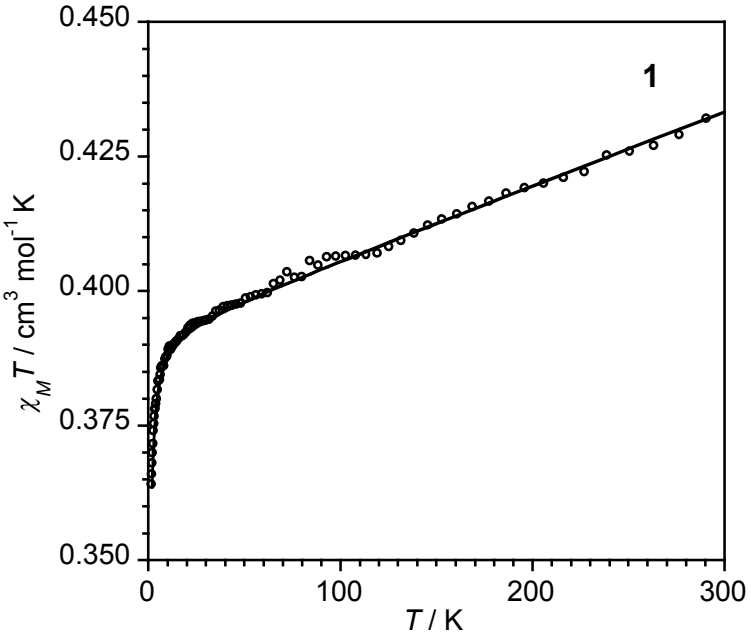

Dalton Transactions Accepted Manuscript

Figure 11. Splitting of the d-metal orbitals for a t_{2g}^5 electronic configuration of a six-coordinate nitrosyl-Re(II) complex under a tetragonal distortion.

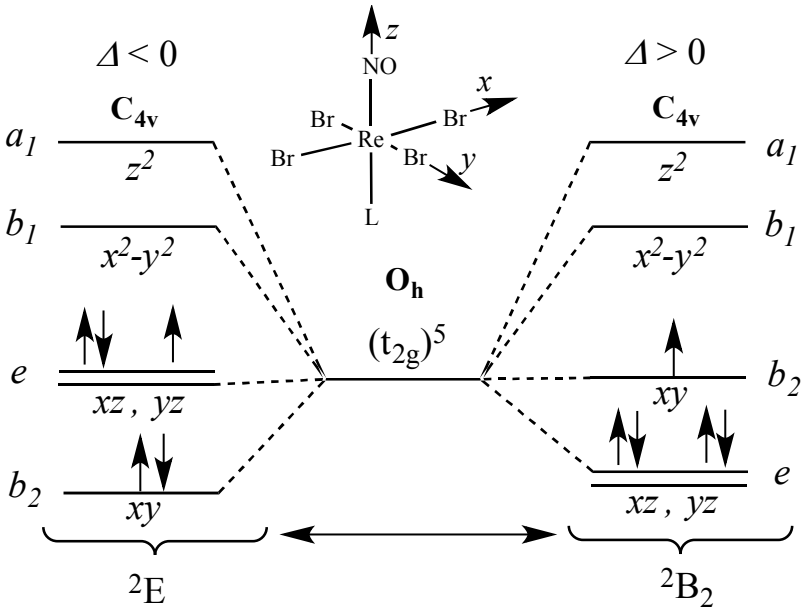

Figure 12. X-band EPR spectrum of a polycrystalline sample of **1** at 4.5 K.

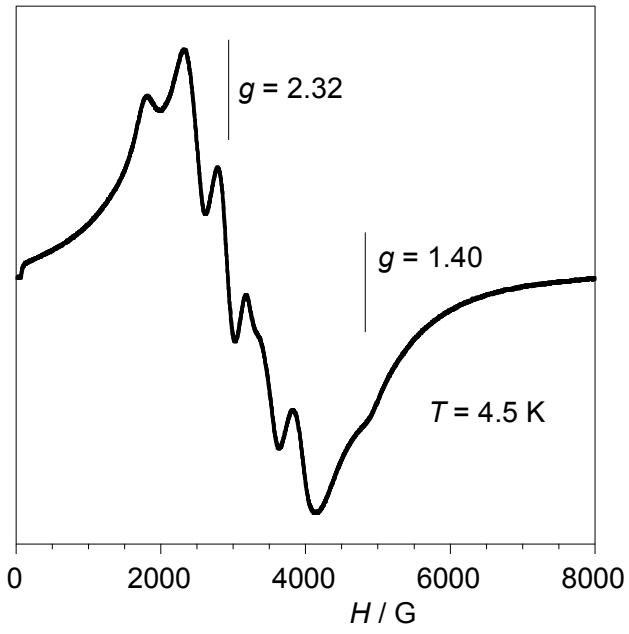

Dalton Transactions Accepted Manuscript

Figure 13. Thermal dependence of the $\chi_M T$ product for **2**: (o) experimental, (—) best-fit curve through eq. (3) (see text).

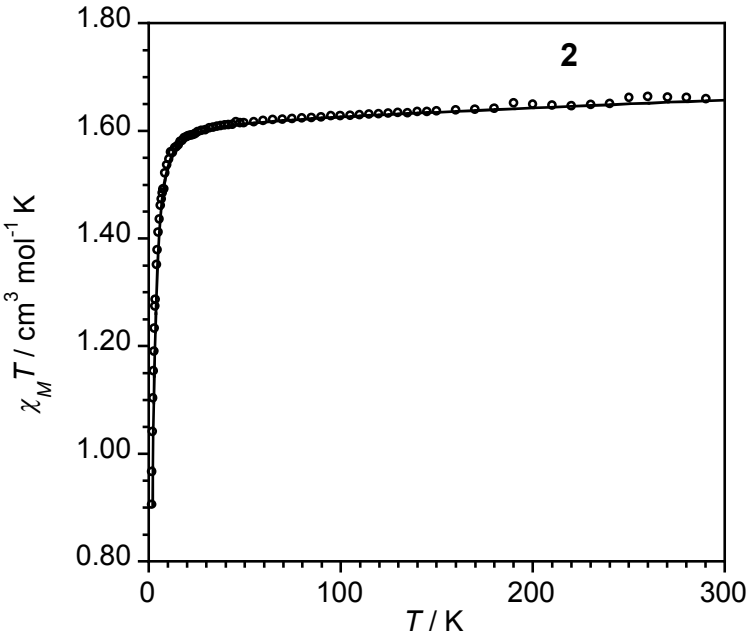

Dalton Transactions Accepted Manuscript

Scheme 1

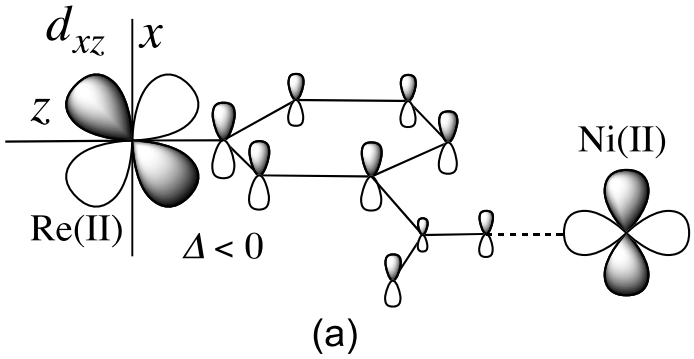

(a)

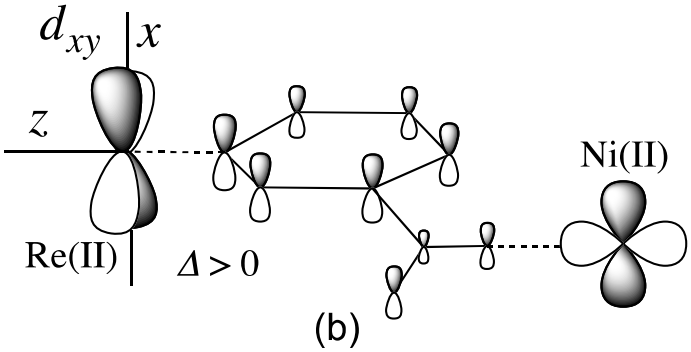

(b)

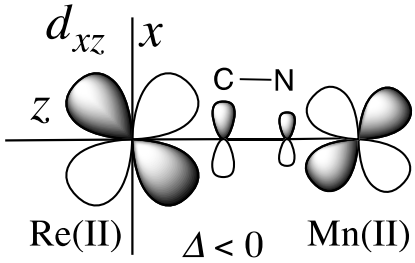

(c)

Dalton Transactions Accepted Manuscript

Contents entry

Five novel complexes $[Re^{II}(NO)Br_4(\mu\text{-nic})M^{II}(L)_2]$ have been prepared and fully characterized. The magnetic properties show a behavior of quasi magnetically isolated spin doublets with very weak antiferromagnetic interactions.

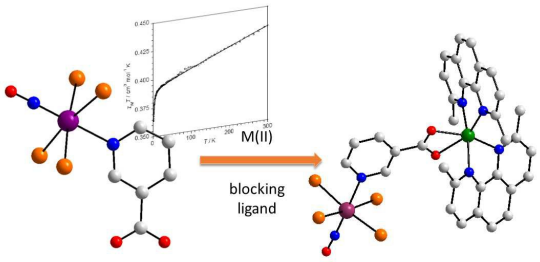

Dalton Transactions Accepted Manuscript